

Intersubband magnetophonon resonances in quantum cascade structures

D. Smirnov^{a†}, O. Drachenko^a, J. Leotin^{a‡}, H. Page^b, C. Becker^b, C. Sirtori^b, V. Apalkov^c, T. Chakraborty^{c*}

^a *Laboratoire National de Champs Magnétiques Pulsés et Laboratoire de Physique de la Matière Condensée, 143 Avenue de Rangueil, 31432 Toulouse, France*

^b *Laboratoire Central de Recherches Thalès, 91404 Orsay, France*

^c *Max-Planck-Institut für Physik komplexer Systeme, 01187 Dresden, Germany*

(October 31, 2018)

We report on our magnetotransport measurements of GaAs/GaAlAs quantum cascade structures in a magnetic field of up to 62 T. We observe novel quantum oscillations in tunneling current that are periodic in reciprocal magnetic field. We explain these oscillations as intersubband magnetophonon resonance due to electron relaxation by emission of either single optical or acoustic phonons. Our work also provides a non-optical *in situ* measurement of intersubband separations in quantum cascade structures.

73.21.Fg,73.43.Qt,85.35.Be,42.55.Px

Ever since the pioneering work on the magnetophonon effect by Gurevich and Firsov [1], high magnetic fields have been regarded as an important tool for investigation of the electron-optical-phonon interaction in semiconductor systems, particularly in confined structures. For the in-plane transport, quantization of the carrier motion in the plane into discrete Landau levels (LLs) of energies $(N + 1/2)\hbar\omega_c$, $\omega_c = eB/m^*$ is the cyclotron frequency, gives rise to quantum oscillations at elevated temperatures due to resonant phonon absorption. These magnetophonon oscillations are periodic in $1/B$, and their strength is related to the electron-optical-phonon coupling, while the period gives either the effective mass or the energy of the participating optical phonons [2]. On the other hand, for perpendicular transport the magnetotunneling measurements in double barrier systems have allowed direct probing of the optical-phonon-assisted transitions from a quasi-two-dimensional (2D) emitter into empty LLs of the central well, as well as determining the effective mass carrier dynamics in these structures [3]. However, little is known from these double barrier studies about intersubband relaxation via optical-phonon emission in quantum wells (QWs). A particularly interesting and unexplored situation occurs when the cyclotron energy exceeds the optical phonon energy and/or the subband energy separation. The first situation is achieved in a GaAs 2D electron gas at magnetic fields above 22 T [2], where the in-plane electron wave function is localized on a scale of the magnetic length, $l_c = \sqrt{\hbar/eB}$ (3.2 nm at 62 T), and the electron behavior is essentially zero dimensional.

Intersubband relaxation via optical phonon emission in quantum wells plays a key role in intersubband radiation sources like the quantum cascade lasers (QCLs) [4]. These systems consist of double-barrier-like structures with three subbands belonging to a central QW structure. When a high bias is applied to the QCL system, the upper subband is populated by tunneling injection.

The electron relaxation in the central wells is then essentially governed by the optical phonon emission rate from both upper subbands. As we demonstrate below, the QCL is appropriate to study intersubband relaxation via optical phonon emission. Recently, intersubband relaxation effects were observed in a GaAs/GaAlAs QC structure from both magnetoresistance and luminescence up to 8 tesla [5]. However, the QCL structure for these studies had intersubband separation much below the LO-phonon energy and therefore, was unable to show resonant relaxation due to optical phonons.

In this paper, we report on our tunneling magnetotransport measurements in a GaAs/GaAlAs QCL structure where a magnetic field of up to 62 T is applied parallel to the current. Our measurements indicate evidence of intersubband magnetophonon oscillations in the tunneling current. These novel oscillations are shown to originate from resonant intersubband relaxation of electrons from the ground state of the upper subband of the central wells into excited Landau level of the lower subbands. A remarkable feature of our results is the lack of dependence of magnetic field positions of these oscillations on the applied bias, as with the in-plane magnetophonon oscillations. These results are supported by theoretical calculations of relaxation rates through acoustic and optical phonons as a function of the magnetic field. An additional benefit of this study is a non-optical *in situ* measurement of intersubband separations in QCL structures.

The n-doped GaAs/GaAlAs QCL structure used for our measurements contains forty periods [6]. Figure 1 shows the results of a self-consistent calculation of the electronic structure along a sequence of the biased QCL sample. The sequence can be depicted like a double barrier tunneling structure including an injector/extractor with five graded gap wells, a wide injection barrier, a three well central zone, and a thin extraction barrier followed by the identical injector/extractor. The energy

levels of the central wells, E_i are indicated by thick horizontal lines in Fig. 1. The emitter on the right hand side of the wide injection barrier behaves as a wide well developing a set of subbands labeled E_n^{inj} , while the collector is a similar well on the left side of the extraction barrier. This picture identifies tunneling from 2D injector/extractor states into/out of 2D active zone states. On the other hand, when a magnetic field is applied perpendicular to the layers, tunneling takes place between 0D degenerate Landau states $E_{i,N}$, localized in a magnetic length scale l_c .

Magnetotransport measurements were performed at 4.2 K on a sample processed into mesa-etched ridge waveguide bars, 20 μm wide and 1.5 mm long. We used a pulsed magnet up to 62 tesla with total duration of 100 ms. The coil is based on a copper-stainless steel wire developed at LNCMP, Toulouse [7]. We have performed mainly magneto-tunneling signal measurements under a fixed DC current or voltage bias. In the following, V^* denotes voltage values across the QCL divided by the number of periods. Fast measurements of $I(V^*)$ curves under quasi-static magnetic fields are also reported. The curves look globally the same when the magnetic field is changed from zero to 62 T as shown in Fig. 2. The current rises in two steps separated by a plateau with a hysteresis behavior. Since the plateaus consist of multiple negative differential segments, this indicates a voltage range where the tunneling transmission is decreasing after a resonant peak. We therefore identify the edge of the plateau as resonant tunneling from E_1^{inj} into $E_{2,0}$ and the second steep rise as beginning of tunneling into $E_{3,0}$ level. The $I(V^*)$ curve profile accounts clearly for the 2D state tunneling.

In what follows, we investigate the quantum oscillations on longitudinal magnetotransport in the bias range well above the hysteresis and current instabilities region. The quantum oscillation extrema are labeled as voltage minima under constant current bias or conversely, as current maxima under constant voltage bias. We limit the bias to the range below 110 mV, where measurements can be made under DC bias without sample thermal drift. Figure 3 (a) shows a typical recording of the oscillatory component of the magnetoresistance of the structure up to 62 T. The second derivative curve is drawn as a dotted line. The inset shows resonance numbers versus the inverse magnetic field given by three curves.

Figure 3 (b) displays the magnetic field positions of oscillation extrema at measured voltage bias V^* applied to the QCL structure. We observe two types of oscillations. The first one occurs mainly in the lower range of bias 75 – 100 mV (12 – 35 mA). In this case, oscillation field positions change roughly linearly with bias as indicated by dashed lines. The curves are drawn with cyclotron energy slopes according to the relation, $eV^* = eV_0^* + N\hbar\omega_c$ for $m^* = 0.07m_0$. The cyclotron energy slope of the oscillation extrema pattern indicates a tunneling transition

from the injector ground state Landau level toward a sequence of excited Landau levels in the central wells. This happens when the tunneling is assisted by the emission of a LO phonon as observed in a magneto-tunneling study of a GaAs/AlGaAs double barrier structure [3].

Let us now consider the second type of oscillations observed in the upper bias range above 100 mV. The oscillation field positions do not change with bias as shown in Fig. 3 (b). Figure 3 (a) shows in the oscillatory component of the voltage across the QCL structure that one series of peaks with the largest amplitude occurs at a fundamental field near 50 tesla. The other two series are also visible on the second derivative curve. All these series are identified in the inset of Fig. 3 (a) which plots integer N versus the reciprocal magnetic field. We label the harmonics in the three series as B_N^i with $i = 1, 2$ and 3 indicating the lower, middle and upper curves respectively. The fundamental fields are obtained from the slopes at the values $B_1^1 = 50$ T, $B_1^2 = 75.5$ T, and $B_1^3 = 95$ T. We can then derive the cyclotron energies $\varepsilon^{(i)} = \hbar e B_1^i / m^*$ by using the effective mass values measured in 2D GaAs electron gas in the same field range as the fundamental fields [8]. We obtain, $\varepsilon^{(1)} = 72$ meV, $\varepsilon^{(2)} = 109$ meV, and $\varepsilon^{(3)} = 149$ meV. Since these energy values are given by the series that are insensitive to the QCL bias, they must be related to the electronic structure of the central wells. In fact, we find $\varepsilon^{(2)}$ and $\varepsilon^{(3)}$ are nearly equal to the photon energies that we measured by the electroluminescence on this structure, namely, 108.7 meV (laser line) and 147 meV (weak luminescence line), respectively. We may then identify the energies $\varepsilon^{(2)}$ as $E_{3,0} - E_{2,0}$ and $\varepsilon^{(3)}$ as $E_{3,0} - E_{1,0}$. The resonance condition for the two series (middle and upper lines in the inset) are then expressed as: $E_{3,0} - E_{2,0} = N\hbar\omega_c$, and $E_{3,0} - E_{1,0} = N\hbar\omega_c$. This corresponds to the elastic transition from the $E_{3,0}$ into an excited Landau level of the other subbands, E_2 and E_1 , respectively.

On the other hand, if one adds the LO-phonon energy (36 meV) to $\varepsilon^{(1)}$, one gets 108 meV, which is close to $E_{3,0} - E_{2,0} = 108.7$ meV. Therefore, the resonance condition for the series corresponding to the lower curve could be $E_{3,0} - E_{2,0} - \hbar\omega_{LO} = N\hbar\omega_c$. This corresponds to an inelastic transition with LO-phonon emission into an excited Landau level of the E_2 subband. A similar inelastic transition is expected into the E_1 subband when $E_{3,0} - E_{1,0} - \hbar\omega_{LO} = N\hbar\omega_c$. In total, one expects four series arising from elastic and inelastic intersubband scattering. However, since in the QCL structure the separation of the lower subbands equals the LO-phonon energy, the elastic response transition from $E_{3,0}$ into $E_{2,N}$ subbands overlaps with the inelastic resonance transition into $E_{1,N}$ subbands. As a result, only three oscillation series should be obtained as found in the experiment.

The observed tunneling current oscillations can indeed be accounted for by resonant intersubband relaxation of electrons with both optical and acoustic phonon emis-

sion. The optical phonon relaxation is possible only if the separation between the levels $\Delta_i = E_3 - E_i - N\hbar\omega_c = \hbar\omega_{LO}$. For the acoustic phonons [9] the resonance in electron relaxation rate occurs when $\Delta_i = \hbar s/l_c$, where s is the speed of sound. Δ_i is about 1 meV at 60 T, which is much less than the intersubband separation.

The rate of electron transition from $E_{3,0}$ into $E_{i,N}$ subbands due to emission of LO or acoustic phonons is

$$\tau_{\mu,i}^{-1} = \frac{2\pi}{\hbar} \sum_j \int \frac{d\vec{Q}}{(2\pi)^3} \delta(\Delta - \hbar\omega_\mu(Q)) (1 + n_{\mu j}(\vec{Q})) \times \left| M_{\mu,j}(\vec{Q}) Z_i(q_z) \right|^2 R_{0N}(q),$$

where index μ stands for optical (LO) or acoustic (A) phonons, $n_{\mu j}(\vec{Q})$ is the phonon distribution function, $\vec{Q} = (\vec{q}, q_z)$ is the three dimensional vector, j labels the phonon mode, $\omega_{LO}(Q) = \omega_{LO}$ and $\omega_A(Q) = sQ$. $M_{\mu j}(\vec{Q})$ are the matrix elements of electron-phonon interaction [10]. For the acoustic phonons we took into account both deformation potential and piezoelectric couplings. The form factors $Z(q_z)$ and $R_{0N}(q)$ are given by the expressions

$$Z_i(q_z) = \int dz e^{iq_z z} \chi_3(z) \chi_i(z),$$

$$R_{0N}(q) = \frac{1}{N!} \frac{(ql_c)^{2N}}{2^N} e^{-(ql_c)^2/2}.$$

To take into account the disorder effect, we introduce the broadening of Landau levels in a Lorentz form with the width of 2 meV and average the relaxation rate over Landau level distribution.

In Fig. 4 (a), the total rate of acoustic phonon emission ($\tau_A^{-1} = \tau_{A,1}^{-1} + \tau_{A,2}^{-1}$) as a function of the magnetic field is shown for $N = 1 - 5$ in units of 10^{10} s^{-1} . In the final state the electron is in $E_{1,N}$ or $E_{2,N}$ Landau ladder. There are sharp resonances when $E_3 - E_2$ or $E_3 - E_1$ is close to $N\hbar\omega_c$. Transitions to $E_{2,3}$ and $E_{1,4}$ are almost at the same magnetic field which is due to the particular structure of the QCL system: subband energies follow the relation, $E_3 - E_2 \approx 3(E_2 - E_1)$, which result in double resonances when the energies of the levels $E_{2,3N}$ and $E_{1,4N}$ are close, where $N = 1, 2, \dots$

In Fig. 4 (b), the total rate of LO phonon emission is shown as a function of the magnetic field for $N = 1 - 5$. Due to the particular structure of the QCL system ($E_2 - E_1 \approx \hbar\omega_{LO}$), resonances due to optical phonons are almost at the same place as the resonances due to acoustic phonons [Fig. 4 (a)]. Finally, in Fig. 4 (c) the total electron relaxation rate ($\tau^{-1} = \tau_A^{-1} + \tau_{LO}^{-1}$) due to emission of acoustic and optical phonons is shown. At $B \approx 25\text{T}$ there are four resonances: two due to the acoustical phonons and the other two due to LO phonons. The model explains the observed resonance field positions fairly well. For example, the oscillation series for transitions to the E_2 subband with optical phonon emission

agree within $\sim 1\%$ with the data for the B_N^1 series, and within $\sim 3\%$ with the data for the B_N^2 series (transitions to the E_1 subband).

In summary, novel magnetophonon oscillation series were observed in the tunneling current across a GaAs/GaAlAs QCL structure. In this system, which behaves like a double-barrier structure, the oscillations originate from resonant intersubband relaxation from the upper subband inside the double-barrier central wells by both optical and acoustic phonons. Magnetic field positions of these oscillations are remarkably independent of the applied bias. The observed results are supported by theoretical calculation of relaxation rates through acoustic and optical phonons as a function of the magnetic field.

We acknowledge helpful discussions with Bruce McCombe. We also acknowledge the cooperation of J. Galibert for the pulsed field measurements and technical support from R. Barbaste and C. Duprat.

* Also at Ioffe Physical Technical Institute, 194021 St. Petersburg, Russia

‡ E-mail: leotin@cict.fr

† Present address: Institute of Mathematical Sciences, Chennai 600113, India

- [1] V.L. Gurevich and Yu.A. Firsov, Zh. Eksp. Teor. Fiz. **40**, 198 (1961) [Sov. Phys. JETP **13**, 137 (1961)]; For a review, see, Yu.A. Firsov, V.L. Gurevich, R.V. Parfeniev and I.M. Tsidil'kovskii, in *Landau Level Spectroscopy*, eds: G. Landwehr, E.I. Rashba (Elsevier, Amsterdam, 1991).
- [2] D.C. Tsui, Th. Englert, A.Y. Cho, and A.C. Gossard, Phys. Rev. Lett. **44**, 341 (1980).
- [3] G.S. Boebinger, A.F.J. Levi, S. Scmitt-Rink, A. Pasner, L.N. Pfeiffer, and K.W. West, Phys.Rev.Lett, **65**, 235 (1990).
- [4] J. Faist, F. Capasso, D.L. Sivco, C. Sirtori, A.L. Hutchinson, and A.Y. Cho, Science **264**, 553 (1994); J. Faist, F. Capasso, C. Sirtori, D.L. Sivco, A.L. Hutchinson, M.S. Hybertsen, and A.Y. Cho, Phys. Rev. Lett. **76**, 411 (1996).
- [5] J. Ulrich, R. Zobl, K. Unterrainer, G. Strasser, and E. Gornik, Appl. Phys. Lett. **76**, 19 (2000).
- [6] P. Kruck, H. Page, C. Sirtori, S. Barbieri, M. Stellmacher, and J. Nagle, Appl. Phys. Lett. **76**, 3340 (2000).
- [7] F. Lecouturier, Thèse de doctorat, Institut National des Sciences Appliquées de Toulouse, 1995; O. Portugal, F. Lecouturier, J. Marquez, D. Givord, S. Askenazy, Physica B **294-295**, 579 (2001).
- [8] S.P. Najda, S. Takeyama, N. Miura, P. Pfeffer, and W. Zawadzki, Phys. Rev. **40**, 6189 (1989).
- [9] P.A. Maksym, in High Magnetic Fields in Semiconductor Physics III, Editor: G. Landwehr (Springer, 1992).
- [10] V.F. Gantmakher and Y.B. Levinson, *Carrier Scattering*

in *Metals and Semiconductors* (North-Holland, Amsterdam, 1987); K.A. Benedict, R.K. Hills and C.J. Mellor, Phys. Rev. B **60**, 10984 (1999); N. Mori and T. Ando, Phys. Rev. B **40**, 6175 (1989); U. Bockelmann and G. Bastard, Phys. Rev. B **42**, 8947 (1990).

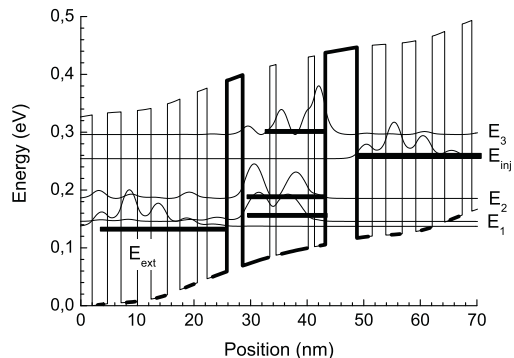


FIG. 1. Electronic structure of a GaAs/GaAlAs QCL sequence with the double-barrier-like profile shown by thick lines. The structure is biased at 117 mV per period. Ground state subband energy levels and their wave functions (squared) for the emitters on the right, central wells, and collectors on the left, are displayed. The layer thicknesses (in nm) along a period starting from the injector on the right toward the central well structure are: 3.6/1.7/3.2/2.2/3.0/2.4/3.0/2.4/2.8/5.6/1.9/1.1/5.8/1.1/4.9/2.8. GaAlAs barriers are shown in bold and the rectangles indicate barriers on both sides of the central well structure with the three subbands E_1 , E_2 , and E_3 . The underline indicates a silicon doped region at a concentration of $6 \times 10^{11} \text{ cm}^{-2}$.

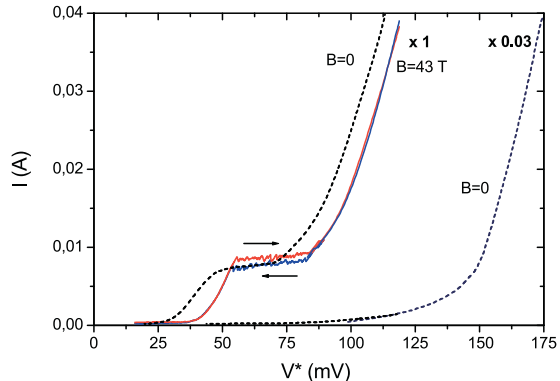


FIG. 2. $I(V^*)$ curves measured at 4.2 K during the up and down voltage ramps at 0 T (dashed line) and 43 T (full line). The two curves correspond to two different scale values on the vertical axis: one for the central curve, and 0.03 for the right curve.

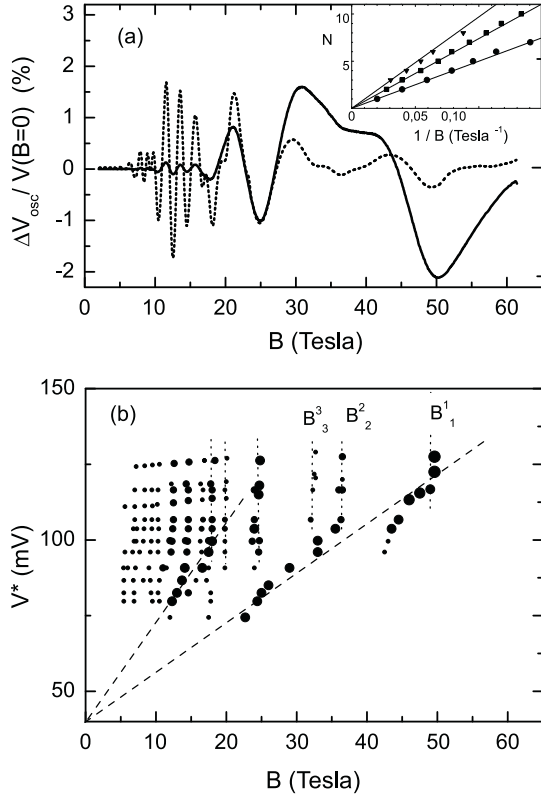


FIG. 3. (a) Oscillatory component of the voltage across the QCL biased at 60 mA and measured in a field of up to 62 T. The second derivative signal is drawn as the dotted line. The inset shows resonance numbers versus the inverse magnetic field, indicated by three series. (b) Oscillation extrema at a given bias. The dot size is related to the oscillation amplitude strength. One type of oscillations is independent of the applied bias, while the other changes roughly linearly with bias. The slope of the dashed line is equal to the cyclotron energy.

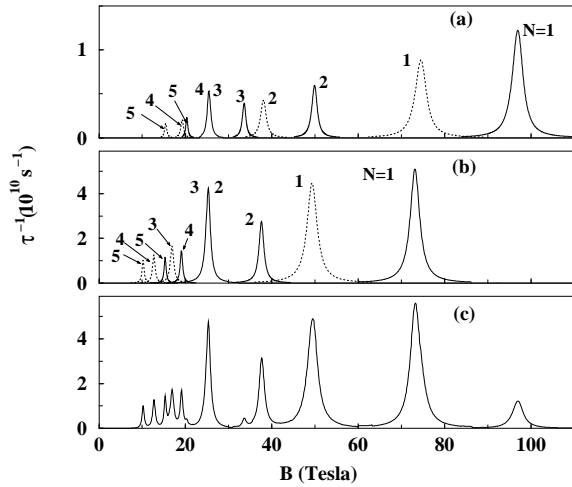


FIG. 4. Acoustic-phonon (a) and LO phonon (b) emission rate as a function of the applied magnetic field. Electron transitions into E_1 and E_2 subbands are shown by solid and dotted lines, respectively. Lines marked by two numbers (4 and 3 in (a) and 3 and 2 in (b)) are the sum of two transitions: into $E_{1,4}$ and $E_{2,3}$ in (a) and $E_{1,3}$ and $E_{2,2}$ in (b). The total electron relaxation rate due to emission of acoustic or optical phonons as a function of magnetic field is shown in (c).